

A Novel Method for the Determination of Cell Infiltration into Nanofiber Scaffolds Using Image Analysis for Tissue Engineering Applications

Dariush Semnani,¹ Laleh Ghasemi-Mobarakeh,¹⁻³ Mohammad Morshed,¹ Mohammad-Hossein Nasr-Esfahani³

¹Department of Textile Engineering, Isfahan University of Technology, Isfahan, Iran

²Islamic Azad University, Najafabad Branch, Isfahan, Iran

³Royan Institute, Isfahan Campus, Tehran, Iran

Received 2 March 2008; accepted 7 July 2008

DOI 10.1002/app.29031

Published online 3 October 2008 in Wiley InterScience (www.interscience.wiley.com).

ABSTRACT: One of the major themes in tissue engineering is scaffold fabrication. The porosity and pore size of scaffolds play a critical role in tissue engineering. Different methods are used to measure the porosity and pore size of scaffolds, although none can predict the cell infiltration for various cell sizes, shapes, and configurations. The aim of this study was to predict the cell infiltration of various cells with different sizes, shapes, and configurations through the use of image analysis. In this study, cell mod-

els were used to predict cell infiltration into nanofiber scaffolds. The results of this study showed that with increases in the cell size and the number of layers of nanofibers, the number of cells that could infiltrate the scaffolds decreased. In addition, the cell configuration had some effect on cell infiltration into the nanofiber scaffolds. © 2008 Wiley Periodicals, Inc. *J Appl Polym Sci* 111: 317–322, 2009

Key words: biofibers; biomaterials; nanotechnology

INTRODUCTION

Tissue engineering has been defined as an interdisciplinary field that applies the principles of engineering and life sciences to the development of biological substitutes that restore, maintain, or improve tissue function.¹ There are generally three key aspects to consider in any tissue-engineered construction: the cells, the scaffold or biomaterial construct, and the cell–material interaction.^{1,2} One of the major themes in tissue engineering is scaffold fabrication. A scaffold is an artificial extracellular matrix that serves as a temporary support in which isolated cells are introduced to form tissue.³ An ideal scaffold for tissue engineering should be highly porous and contain an interconnected pore network through which nutrients and metabolic waste can flow. In addition, it should be biodegradable via a readily controllable mechanism, have suitable surface properties (chemical and physical) for initial cell attachment, and be easily processed to form a variety of shapes and sizes.⁴ Generally, the hydrophilic/hydro-

phobic character of the scaffold is important in tissue cultures and can influence initial cell adhesion and cell migration, proliferation, and differentiation. To enhance the biocompatibility of polymeric nanofiber scaffolds, surface modifications of the scaffolds via plasma treatment or coating with hydrophilic polymers, such as poly(ethylene oxide) and poly(vinyl alcohol), have been examined. The roughness of the scaffold surface also influences the initial cell attachment and cell proliferation.⁴

The surface properties of biomaterials are a key aspect in determining compatibility with the biological environment and cellular responses. Ideally, scaffolding materials should be designed to be bioactive so that they can receive and respond to specific biological signals, which will direct and promote cell attachment, proliferation, differentiation, and tissue regeneration.⁵

The porosity and pore size of scaffolds play critical roles in tissue engineering.⁶ A scaffold should have high porosity and a proper pore size to permit the ingress of cells and nutrients.^{1,7-9} Adequate porosity and surface area are widely recognized as important parameters in the design of scaffolds for tissue engineering.¹⁰ A large pore volume is required to accommodate and subsequently deliver a cell mass sufficient for tissue repair.⁷ The pores of scaffolds are very important for cell growth. The cells adhere to the surface of the scaffolds, absorb

Correspondence to: M. Morshed (morshed@cc.iut.ac.ir).

Contract grant sponsors: Textile Department, Isfahan University of Technology.

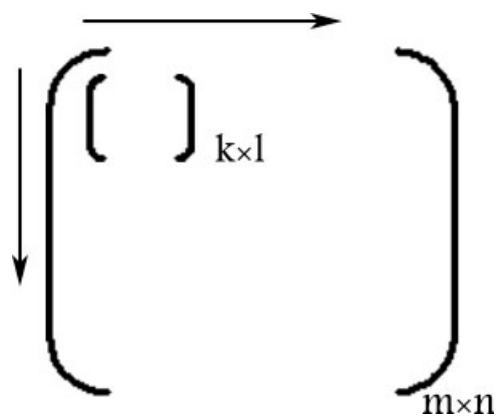


Figure 1 Movement of the mask matrix through the matrix of nanofiber mat.

nutrients, and remove metabolites through the pores.¹¹ The diameter of cells in a suspension dictates the minimum pore size, which varies from one cell type to another and must be controlled carefully.^{7,12} If the pores are too small, the cells cannot enter, and if they are too large, the cells cannot adhere.¹¹

Different methods are used to measure porosity and pore size in scaffolds. Mercury intrusion porosimetry is a method used to measure both porosity and pore size. The advantages and disadvantages of this method have been explained in a previous study.¹³ In brief, the main advantage of this method is the ability to measure the pore size and its distribution, the total pore volume, and the total pore area.¹⁴ A major drawback of using mercury porosimetry is that generally very high pressures are required as the pore size diminishes. Therefore, when thin sections are analyzed, there is a high possibility that the membrane will be destroyed at higher pressures. This is especially true for electrospun nanofibrous membranes because the pores in electrospun membranes are not rigid enough. The other drawbacks of using mercury are its cost and toxicity.¹⁴ Scanning electron microscopy (SEM) images are analyzed with various computer programs to measure porosity and particularly pore size. Finally, microcomputed tomography imaging and analysis have been used to determine porosity and pore size in three-dimensional scaffolds.⁴ Because various cells have different shapes and sizes,¹⁵ the appropriate pore size is different for various cell types. For example, for the scaffold used for the knee meniscus, it has been reported that the pore size should be at least 30 μm for the ingrowth of tissue before scaffold degradation, and pore sizes of 150–355 μm have been recommended for healing of the meniscus lesion situated in the

vascular part of the meniscus and fibrocartilaginous tissue developing inside the implants.¹⁶

The aforementioned methods cannot determine the ability of cell infiltration for various cell shapes and configurations.

It must be emphasized that although biodegradable porous scaffolds with well-interconnected pores are good enough to permit cell infiltration and growth, their surface characteristics arising from their chemical composition, such as hydrophilicity/hydrophobicity, may not be satisfactory for inducing selective cell adhesion, migration, and proliferation.¹⁷

In a previous study,¹³ we investigated the porosity of various visible layers of nanofiber scaffolds using image analysis. The results revealed that image analysis can easily be applied to the porosity measurement of various layers. The aim of this study was to predict the infiltration of cells of various sizes and shapes into nanofiber scaffolds with image analysis. As in the previous study, an electrospinning method was used to produce electrospun poly(ϵ -caprolactone) (PCL) nanofiber scaffolds, and a novel image analysis procedure was applied to the prediction of the infiltration of cells of various sizes and shapes into nanofiber scaffolds.¹³

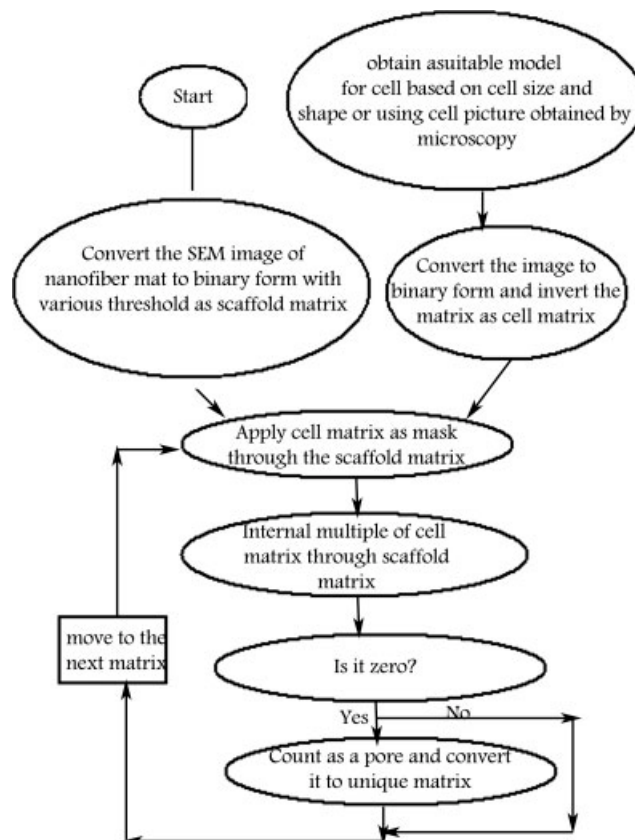


Figure 2 Diagram of the stages for the determination of cell infiltration ability through the scaffold.



Figure 3 Model for a circular shaped cell with a diameter of 10 μm : (A) primary and (B) inverted images.

EXPERIMENTAL

Materials

PCL (number-average molecular weight = 80,000) was purchased from Aldrich (Sigma-Aldrich, St. Louis, MO). Methylene chloride and dimethylformamide were purchased from Merck Co. (Germany).

PCL nanofiber scaffolds were produced by an electrospinning method. The method was previously explained.¹³ In brief, a polymer solution with a concentration of 10 wt % was prepared by the dissolution of PCL in a solvent mixture of methylene chloride and dimethylformamide with the ratio of 80/20, and electrospinning was carried out from a 10-mL syringe with a needle diameter of 0.6 mm and by the application of a high voltage of 12 kV

with a mass flow rate of 4 mL/h toward a target that was placed 20 cm from the syringe tip.

Methodology

The SEM photographs of the nanofiber mat were scanned with an Hewlett-Packard Scanjet 3670 scanner. The resolution of the scanned images was 600 dpi, and the gray-scale level was 256. This scanning resolution was determined by experimental observation. A lower resolution made the analysis poor, whereas a higher resolution did not improve the analysis results and caused a reduction in the analysis speed. According to the previous study,¹³ the threshold was determined, and the pore sizes at various visible layers were measured. After the conversion of a gray-scale image to a binary form with a suitable threshold, a novel image analysis technique was sought to determine whether a cell could infiltrate the scaffold or not. In this research, a novel method of object reorganization was applied. There are two objects of cells and pore spaces that should be investigated for shape conformity. Some methods of box counting, such as fractal analysis, have been tried to analyze the shapes of pore spaces.^{18,19} The fractal method lacks sufficient precision and cannot be used for circular or oval shapes of various cells because of the rectangular shape of the assessing object in these methods. Because of the drawbacks of the fractal method, a more applicable method for

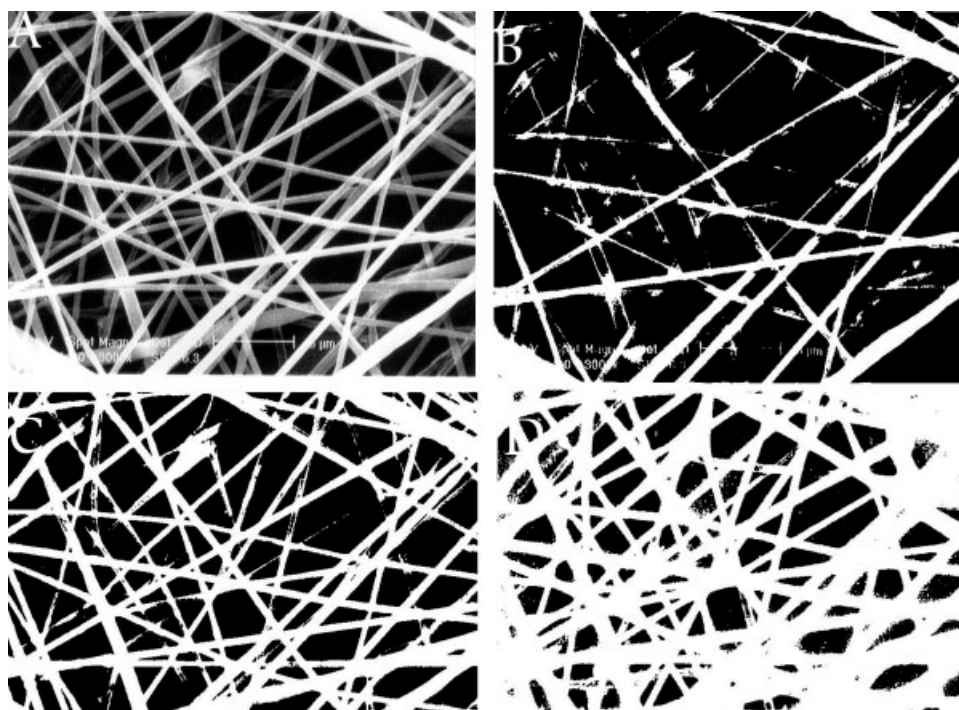


Figure 4 Various binary images with different thresholds: (A) original image, (B) binary image with a threshold of $(\mu + \sigma)/255$, (C) binary image with a threshold of $\mu/255$, and (D) binary image with a threshold of $(\mu - \sigma)/255$. μ and σ are the mean and standard deviation of the image matrix, respectively.

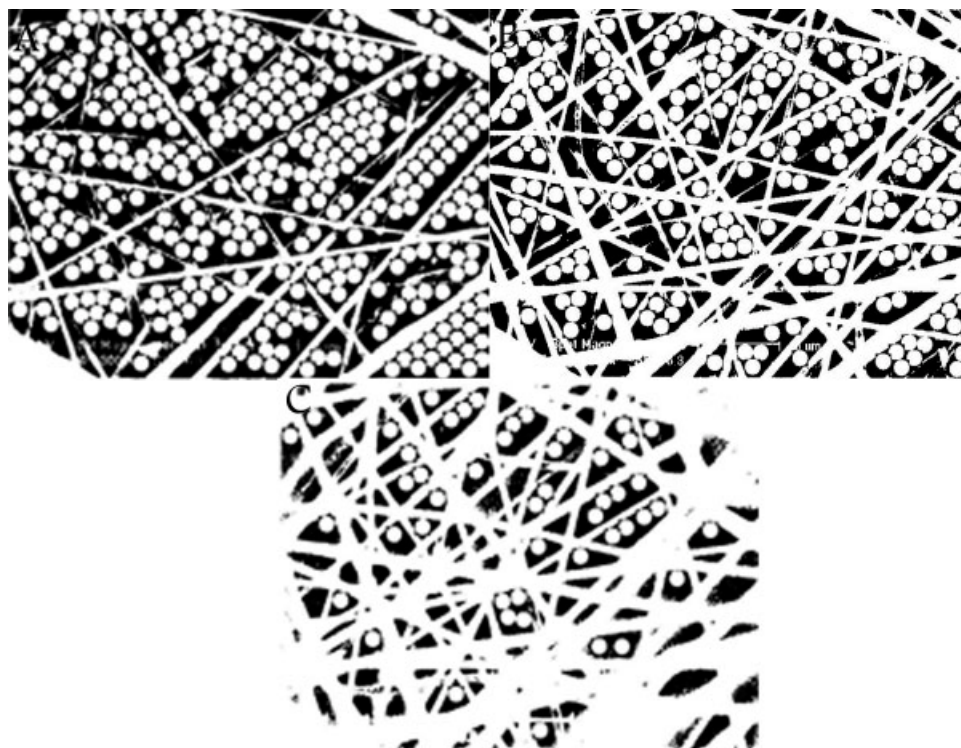


Figure 5 Various binary images with different thresholds: (A) Figure 4(B), (B) Figure 4(C), and (C) Figure 4(D) after the application of the mask matrix related to the cell with a circular shape and a diameter of 10 μm .

the determination of the infiltration of various cells with different sizes and shapes was developed in this research.

A picture of a cell can be obtained by microscopy, and because different cells have different shapes and sizes depending on the cell type, a suitable model can be defined by the drawing of the cell with suitable software.

After the image of a cell is obtained by drawing or microscopy, the image is converted to a binary form with a threshold of 0.5 in the intensity image of the cell. The fibers and pore spaces appear as white and black pixels, and the cell image is drawn as black pixels; the cell image should be inverted to white pixels. Therefore, the matrix related to the cell image is inverted before its application through the SEM image of the nanofiber mat as a mask matrix. With an internal multiple mask and the matrix of the SEM image of the nanofiber mat, the pores can be recognized. In the pore spaces, the internal multiple mask and main matrix are equal to a zero matrix. If the matrix produced from the internal multiple mask matrix and the main matrix is equal to zero, then the space will be recognized as a pore. To prevent the overcounting of pores, after the recognition of pores, it must be changed to a 1s matrix (white pixels), and therefore it is not counted again. By the movement of the mask matrix through the matrix of the SEM image of the nanofiber mat, the pores can be counted.

If the size of the matrix is related to the binary image of the nanofiber mat (matrix \mathbf{M}) and cell image (matrix \mathbf{J}), which are to be taken as $m \times n$ and $k \times l$, respectively, then the cell image matrix can be applied to the matrix of the nanofiber mat vertically and horizontally according to Figure 1. The mask matrix moves through the matrix, which is related to the nanofiber matrix pixel by pixel, and for each pixel, the mask matrix is applied to this pixel and its neighborhood with dimensions of $k \times l$.

In each step of applying the mask to the image matrix, T is defined as follows:

$$T = \sum_{i=1}^k \sum_{j=1}^l \mathbf{M}_{i,j} \mathbf{J}_{k,l} \quad (1)$$

If T is equal to zero, then the space under matrix \mathbf{J} will be a pore and will be counted as a pore. To

TABLE I
Number of Cells with Various Sizes and Circular Shapes That Could Infiltrate the Scaffolds













Cell diameter (μm)	10	20	30
Shape of cell			
Threshold			
$(\mu + \delta)/255$	344	51	8
$\mu/255$	173	12	0
$(\mu - \delta)/255$	48	0	0

TABLE II
Number of Cells with Various Sizes and Configurations and Oval Shapes That Could Infiltrate the Scaffolds

Cell diameter (μm)	10	10	10	20	20	20	30	30	30
Shape of cell									
Threshold									
$(\mu + \delta)/255$	1591	1461	2877	297	242	384	88	61	133
$\mu/255$	915	789	1386	116	91	144	20	14	25
$(\mu - \delta)/255$	305	259	428	23	7	30	0	0	6

prevent overcounting, the recognized pore should be changed to 1s so that it will not be counted again; T will not be zero in the next step of applying the mask to the image matrix.

Figure 2 shows schematically the procedure determining the ability of cell infiltration through the scaffold.

RESULTS AND DISCUSSION

In this study, various models for cells were used. It should be kept in mind that the image size must be obtained with respect to the magnification of the SEM image of the nanofiber mat and that the same resolution of the SEM image is needed for the image of the cell. For example, for an SEM image of a nanofiber mat with a magnification of 3000, a cell with a circular shape and diameter of $10 \mu\text{m}$ must be drawn with a diameter of $10 \times 3000 \times 10^{-4} = 0.3 \text{ cm}$.

Figure 3(A) shows a model for a circular cell with a diameter of $10 \mu\text{m}$. After the conversion of the image to a binary form, it is inverted. Figure 3(A,B) shows the main and inverted versions of the image, respectively.

By the application of the matrix related to Figure 3(B) as a mask through the matrix of the SEM image of the nanofiber mat and the internal multiple, pores can be recognized.

Figure 4 shows various binary images of nanofiber mats with different thresholds, and Figure 5 shows the binary images after the application of the mask matrix related to cells with a circular shape and a diameter of $10 \mu\text{m}$.

As can be seen in Figure 5, with an increase in the number of layers, the number of cells that can diffuse into the scaffolds decreases. The reduction of cell infiltration into the nanofiber scaffolds is due to the increase in the number of layers, as explained in the previous study.¹³ Tables I and II show the number of cells with circular and oval shapes and diameters of 10, 20, and $30 \mu\text{m}$ that can infiltrate various visible layers.

As can be seen in Tables I and II, with an increase in the number of layers and cell size, the number of cells that can infiltrate the scaffolds decreases, and when the diameter of the cells increases to $30 \mu\text{m}$,

the cells cannot diffuse anymore into the inner layers of the nanofiber scaffolds. These results are consistent with other research. According to the other research, the cells cannot penetrate the nanofiber scaffolds because of the small sizes of the pores of the nanofiber scaffolds.²⁰⁻²³ In addition, the shapes and configurations of cells are effective parameters for cell infiltration. For example, the infiltration of oval cells with a large diameter of $10 \mu\text{m}$ is more than that of circular cells with the same diameter.

The procedure for SEM images of nanofiber scaffolds with different magnifications is the same, but in the cell modeling, the magnification must be taken into account or the obtained microscopy pictures must have the same magnification. For example, for an SEM image of a nanofiber mat with a magnification of 6000, with a circular cell and a diameter of $10 \mu\text{m}$, the cell model must be drawn with a diameter of $10 \times 6000 \times 10^{-4} = 0.6 \text{ cm}$.

The main advantage of the procedure presented in this research is its ability to determine the cell infiltration of various cell types into the various layers of nanofiber scaffolds, whereas with the other methods presented in previous studies, only the pore size and its distribution could be determined. On the other hand, with this method, with knowledge of the sizes and shapes of cells, appropriate models can be defined, and cell infiltration can be predicted.

CONCLUSIONS

With the aid of image analysis, we explored the possibility of predicting cell infiltration into nanofiber scaffolds for various cells with different cell sizes, shapes, and configurations. The results of this investigation revealed that image analysis can easily be applied to determine cell infiltration into nanofiber scaffolds. The measurements by such a simple method can be applied to applications such as scaffolds for tissue engineering in which the pore sizes are very important. The porosity measurements based on the other methods cannot predict cell infiltration for various cell shapes and configurations and can determine only the pore size of nanofiber scaffolds.

The results of this study show that with increases in the cell size and the number of layers of nanofibers, the number of cells that can infiltrate scaffolds decreases, and when the diameter of cells increases to 30 μm , the cells cannot diffuse into the inner layers. In addition, the cell configuration has a major effect on cell infiltration into nanofiber scaffolds.

The authors thank Maryam Karbasi for performing the SEM tests.

References

1. Ma, P. X. *Mater Today* 2004, 7, 30.
2. Murugan, R.; Ramakrishna, S. *Tissue Eng* 2006, 12, 435.
3. Papenburg, B. J.; Vogelaar, L.; Bolhuis-Versteeg, L. A. M.; Lammertink, R. G. H.; Stamatialis, D.; Wessling, M. *Biomaterials* 2007, 28, 1998.
4. Kim, G.; Park, J.; Park, S. *J Polym Sci Part B: Polym Phys* 2007, 45, 2038.
5. Liu, X.; Won, Y.; Ma, P. X. *J Biomed Mater Res A* 2005, 74, 84.
6. Karageorgiou, V.; Kaplan, D. *Biomaterials* 2005, 26, 5474.
7. Ma, Z.; Kotaki, M.; Inai, R.; Ramakrishna, S. *Tissue Eng* 2005, 11, 101.
8. Yang, S.; Leong, K. F.; Du, Z.; Chua, C. K. *Tissue Eng* 2001, 7, 679.
9. Shobana, S. A. M.S. Thesis, New Jersey Institute of Technology, 2004.
10. Gomes, M. E.; Holtorf, H. L.; Reis, R. L.; Mikos, A. G. *Tissue Eng* 2006, 12, 801.
11. Shi, G.; Cai, Q.; Wang, C.; Lu, N.; Wang, S.; Bei, J. *Polym Adv Technol* 2002, 13, 227.
12. Buckley, C. T. In *Topics in Bio-Mechanical Engineering*; Prendergast, P. J.; McHugh, P. E., Eds.; Trinity Centre for Bioengineering and the National Centre for Biomedical Engineering Science: Dublin and Galway, 2004; Chapter 5.
13. Ghasemi-Mobarakeh, L.; Semnani, D.; Morshed, M. *J Appl Polym Sci* 2007, 106, 2536.
14. Ramakrishna, S.; Fujihara, K. *An Introduction to Electrospinning and Nanofibers*; World Scientific: River Edge, NJ, 2005; Chapter 5.
15. Junqueira, L. C.; Carneiro, J. *Basic Histology: Text & Atlas*, 8th ed.; Editora Guanabara Koogan: Rio de Janeiro, 2005; Chapter 9; World Scientific Publishing Co. Pte Ltd. (Jun 2005), printed in Singapore by World Scientific printers(S) Pte Ltd.
16. Lee, Y. H.; Lee, J. H.; An, I. G.; Kim, C.; Lee, D. S. *Biomaterials* 2005, 26, 3165.
17. Chung, H. G.; Park, T. G. *Adv Drug Delivery Rev* 2007, 59, 249.
18. Sul, I. H.; Hong, K. H.; Shim, H. S.; Kang, T. J. *Text Res J* 2006, 76, 828.
19. Yang, X.-H.; Li, D.-G. *J Dong Hua Univ* 2005, 22, 103.
20. Pham, Q. P.; Sharma, U.; Mikos, A. G. *Biomacromolecules* 2006, 7, 2796.
21. Chong, E. J.; Phan, T. T.; Lim, I. J.; Zhang, Y. Z.; Bay, B. H.; Ramakrishna, S.; Lim, C. T. *Acta Biomater* 2007, 3, 321.
22. Townsend-Nicholson, A. N.; Jayasinghe, S. *Biomacromolecules* 2006, 7, 3364.
23. Kim, G.; Kim, W. *J Biomed Mater Res B* 2007, 81, 104.